Hindawi
Advances in Meteorology
Volume 2018, Article ID 9256396, 12 pages
https://doi.org/10.1155/2018/9256396

Research Article

Impact of Using Near Real-Time Green Vegetation Fraction in Noah Land Surface Model of NOAA NCEP on Numerical Weather Predictions

Li Fang,[1,2] **Xiwu Zhan**,[2] **Christopher R. Hain**,[3] **and Jicheng Liu**[1,2]

[1]*Earth System Science Interdisciplinary Center, University of Maryland, 5825 University Research Court, College Park, MD 20740, USA*
[2]*NOAA/NESDIS/STAR, 5830 University Research Court, College Park, MD 20740, USA*
[3]*NASA Marshall Space Flight Center, Redstone Arsenal, Huntsville, AL 35812, USA*

Correspondence should be addressed to Li Fang; li.fang@noaa.gov

Received 3 January 2018; Revised 23 March 2018; Accepted 11 April 2018; Published 5 June 2018

Academic Editor: Qingyan Meng

Green vegetation fraction (GVF) is one of the input parameters of the Noah land surface model (LSM) that is the land component of a number of operational numerical weather prediction (NWP) models at the National Centers for Environmental Prediction (NCEP) of NOAA. The Noah LSM in current NCEP operational NWP models has been using static multiyear averages of monthly GVF derived from satellite observations of NOAA Advanced Very High Resolution Radiometer (AVHRR) normalized difference vegetation index. The multiyear averages of GVF are evidently not the representative of actual conditions of the land surface vegetation cover. This study used a near-real-time (NRT) GVF data set generated from the 8-day composite of the leaf area index product from the Moderate Resolution Imaging Spectroradiometer (MODIS) to assess the impact of NRT GVF on off-line Noah LSM simulations and NWP forecast model. Simulations of the off-line Noah LSM in the Land Information System (LIS) and weather forecasts of the NASA-Unified Weather and Research Forecasting (NUWRF) were obtained using either the static multiyear average AVHRR GVF data set or the NRT MODIS GVF while meteorological forcing data and other settings were kept the same. The off-line simulations and WRF forecasts were then compared against in situ measurements or reanalysis products to assess the impact of using NRT GVF. Improvements of both soil moisture simulations as well as forecasts of 2-meter air temperature and humidity and precipitation from NUWRF were observed using the NRT GVF data products. The RMSE in SM estimates from the off-line Noah model is reduced by around 1.0% (1.41%) during the green-up phase and by 1.48% (2.24%) over the senescence phase for the surface (root zone) SM simulations. Around 82.3% validation sites (out of 1178 sites) showed positive impact on coupled WRF model with the insertion of NRT GVF.

1. Introduction

Comprehensive land surface models are routinely used in the North American Land Data Assimilation System (NLDAS) and are widely employed to support weather prediction studies, water and energy cycle investigation, and the research in land surface processes on climate extremes [1–5]. The reliabilities of these applications are greatly affected by the uncertainties in model parameters and forcing inputs [6, 7]. For instance, the exchange of energy and water fluxes in operational LSMs is sensitive to the green vegetation fraction (GVF), an important weighting coefficient in partitioning total evapotranspiration into the three components of evaporation [7, 8]. However, the GVF inputs employed in the current NLDAS framework are multiyear climatology derived from the Advanced Very High Resolution Radiometer (AVHRR) [8, 9]. Evidently, the static climatological maps are not always the representative of the

actual conditions of the land surface vegetative cover [6, 10–14]. On another aspect, many vegetation products are becoming increasingly available from remote sensing platforms, which are capable of providing more representative situation of the current land surface vegetation state. Among all the sensitive surface forcing inputs and parameters to the Noah LSM, this research aims at assessing the impact of near real-time (NRT) GVF, as one of the essential parameters on the surface energy balance and energy exchange, on both off-line land surface model and numerical weather prediction (NWP) model.

Although GVF climatology derived from AVHRR has been operationally used in the numerical weather forecasting models for a wide range of applications, the representativeness issues and improvements are worth discussing. Most importantly, surface vegetation cover could be highly variable annually and seasonally [15]. Therefore, the multiyear average maps would miss the intra- and interannual variability of the real surface vegetation condition, which could lead to misinterpolating surface energy partitioning and exchange. The NRT GVF, on the other hand, which can be derived from remotely sensed observations with high temporal resolution, is expected to capture the reality, especially during fast changing growing seasons. An improved representation of surface vegetation cover may provide improvements to simulations from off-line LSMs and could potentially lead to significant forecast improvements as well.

Some studies have addressed the weakness of static climatological parameters [6], while others have attempted to replace the old climatology with new "real-time" weekly or monthly GVF into land surface and/or NWP models [10–14]. Miller et al. [14] and Ruhge and Barlage [11] have conducted sensitivity analysis of real-time GVF (MODIS-based) on off-line Noah LSM. Yin at al. [10] examined the impact of both NRT albedo and GVF. They concluded that the use of NRT GVF improved Noah surface soil moisture simulations by 19.3% and surface soil temperature by 9.3%. James at al. [13] investigated the value of real-time GVF when incorporated into a 2 km nested Advanced Research Weather Research and Forecasting (ARW) model. Jiang at al. [12] generated a new operational real-time weekly GVF data set from AVHRR observations. They further tested the use of the new product in the Noah LSM and NWP models, and impacts were concluded as overall positive. Although current research has shown the positive value of real-time GVF for land surface and weather forecast models, those studies are either based on the limited period of time or validated at local scales. The primary objectives of this study are to verify the impacts of NRT GVF on off-line LSM simulations for a long-term run and NWP forecasts over conterminous U.S. (CONUS).

The outline of this paper is as follows. Section 2 introduces land surface models and frameworks involved in this study, followed by detailed description of experiment setup. The introduction to climatology and NRT GVF data sets and relevant validation data sets is given in Section 3. In Section 4, impacts of NRT GVF on off-line Noah soil moisture (SM) simulations and weather forecasts from a NWP model are evaluated. The benefits of using NRT GVF are assessed by comparing the estimates from LSM and forecasts from NWP against field measurements. Further work and conclusions are summarized in Section 5.

2. Land Surface and Numerical Weather Prediction Model

2.1. Noah LSM and LIS Implementation. The NASA Land Information System (LIS) is a flexible software framework to integrate satellite and ground-based observations and major LSMs to accurately characterize land surface states and fluxes [16, 17]. The land surface modeling infrastructure in LIS consists of several well-documented LSMs (Noah, CLM, Catchment, Mosaic, etc.), which typically run in an uncoupled mode using a combination of observationally based precipitation, radiation, meteorological, and land surface parameter data sets. The Noah LSM implemented within LIS is used in this study for all the numerical experiments because it is employed in the operational land surface modeling component for the numerical weather prediction at the National Center for Environmental Prediction (NCEP) [15, 18]. The Noah LSM is a one-dimensional soil-atmosphere-vegetation transfer model which simulates four-layer soil moisture (both liquid and frozen) with the thicknesses of 0–0.1, 0.1–0.4, 0.4–1, and 1–2 m [2, 15, 18, 19]. Specifically, Noah model version 3.3 is adopted in LIS from off-line simulations, and it severs as the core land component in the standard NCAR Advanced Research Weather and Research Forecast (WRF-ARW) model for weather forecasting.

2.2. LIS Semicoupled with WRF. The NASA-Unified WRF (NUWRF) modeling system developed at NASA Goddard Space Flight Center (GSFC) is an observation-driven integrated modeling system representing aerosol, cloud, precipitation, and land processes at satellite-resolved scales [20]. The NUWRF (version 7) adopted in this study incorporates the standard NCAR Advanced Research WRF (ARW) version 3.5.1 and LIS (v7.0rp1) into a unified framework with distinct advantages of (1) setting up long-term spin up land surface conditions on the common grid as the WRF forecast domain; (2) providing LIS land simulations with near surface forcing from the parent WRF run; and (3) easy replacement of updated initial conditions from LIS output to WRF. To be consistent, Noah LSM version 3.3 severs as the core land component in the standard WRF-ARW model for forecasting. In this study, the semicoupled LIS/WRF workflow is selected to test the impact of NRT GVF insertion on WRF weather forecast. In the coupling workflow, WRF provides atmospheric forcing data to LIS, and LIS sets up the simulation domain on the same grid (spatial resolution and projection) with the same terrestrial data and land surface physics (identical versions of the Noah LSM) as WRF run. The replacement of NRT GVF is conducted within LIS. LIS then generates updated initializations daily and returns updated initial land surface data (e.g., vegetation cover, SM, soil temperature, fluxes, and albedo) to WRF for next day forecasts.

Table 1: LIS-WRF model configuration details.

Variables	Assignment
WRF dynamical core	Advanced research WRF
Grid spacing/projection	12 km/Gaussian
Dimension (west-east by south-north)	480 ∗ 400
Integration time step	24 s (the same in LIS and ARW)
Vertical dimension	30
Number of soil layers	4
Land cover type	MODIS (20 category)
GVF	Climatology: AVHRR, 0.144 degree NRT: MODIS, 1 km
Microphysics	5 (Eta microphysics: the operational microphysics in NCEP models)
Land surface model	Noah (v3.3)
Planetary boundary layer	Mellor–Yamada–Janjic scheme

2.3. Experiments on Off-Line Noah and NUWRF Models. Impacts of NRT satellite-based GVF are assessed on both off-line Noah LSM and WRF-ARW. As for the off-line LSM, the benefit over a long-term period (13 years) is analyzed. Noah LSM simulations are performed from 2000 to 2012, using climatological data sets and NRT satellite observations separately with identical meteorological forcing data. As for the NWP model, this study targets at a 2-week period from 27 September to 10 October 2015 when semicoupled LIS/WRF runs are set up to run with climatology GVF and NRT GVF separately while keeping settings of model grid, physical process schemes, and boundary conditions the same. More details of experiment settings for the off-line Noah LSM and NWP model are given in the following sections.

2.3.1. Experiment on Off-Line Noah LSM. To demonstrate the benefit of NRT satellite-based GVF, two off-line Noah simulations are performed, one using standard 5-year average GVF maps as model inputs (Noah-clim run) and the other with NRT GVF (Noah-NRT run). The Noah-clim run serves as the benchmark for the quantification of improvement or degradation with replacement of NRT GVF (Noah-NRT run). The Noah simulations are forced by the NLDAS-2 forcing [21, 22], which provides long-term model- and observation-based hydrological and meteorological data sets on a common grid at 1/8° spatial resolution and hourly temporal resolution. The study domain is set to be consistent with operational NLDAS domain, covering the contiguous United States at 0.125° spatial resolution with the validation period extending from 2000 to 2012. The Noah model is integrated forward using a 30-minute time step and outputs daily SM fields (in volumetric $m^3 \cdot m^{-3}$ units) for analysis. In order to create realistic initial variability in SM states, the land profile is uniformly initialized and "spin-up" for a period from 1 January 1999 to 31 December 2012, and all the simulations are initialized at 1 January 1999 with the analysis field from "spin-up" on the day 31 December 2012 and rerun through 31st December 2012. Soil moisture estimates of those two simulations (Noah-clim and Noah-NRT runs) are then compared against a collection of in situ SM measurements to evaluate NRT GVF's impact.

2.3.2. Experiment on Weather Forecast Model. Two LIS/WRF simulation experiments are set up to evaluate the impact of NRT GVF on the weather forecast model. One is an open-loop run using climatology GVF (WRF-clim), and the other WRF run (WRF-NRT) is set up with the insertion of NRT GVF. WRF-clim run will be the reference to assess the impact of the NRT GVF on land-atmosphere coupling. In WRF-NRT run, initializations of land states are updated with the replacement of NRT GVF. The daily updated land states will impact the subsequent forecasts in response to the changes in surface GVF.

The study domain is set up at 12 km spatial resolution in the Gaussian projection covering Northern America. The LIS-WRF runs are conducted for 14 days from 27 September to 10 October 2015. From 3 October, WRF forecasts for each time step (4 steps a day for 7 days) are used to evaluate the impacts of NRT GVF. Each model run is set up for 48-hour forecasts, with hourly outputs starting from a fixed initialization time (0600 UTC). The 6-hour GFS data are selected as forcing data to initialize the ARW model runs. The model configuration is summarized in detail in Table 1. The settings of the model grid, physical process schemes, and boundary conditions are kept the same in WRF run with climatology and NRT GVF data sets.

3. Data Sets

3.1. Climatology and Near Real-Time GVF Data Sets. The climatology GVF data set used in current NCEP operational Noah LSM is 5-year (1985–1989) average derived from AVHRR observations. It provides monthly specification of GVF with the spatial resolution of 0.144° in a latitude-longitude projection [8].

The NRT GVF data used in this study are derived from the 1 km MODIS/Terra 8-day composite LAI product (MOD15A2, V005) with the following equation:

$$\mathrm{GVF} = 1 - e^{-b*\mathrm{LAI}}, \quad (1)$$

where $b = 0.5$ is the extinction coefficient for general plant canopy [23]. LAI in this equation is from the standard MODIS LAI and FPAR product (MOD152A, V005) derived at 1 km from MODIS spectral reflectance for all vegetated

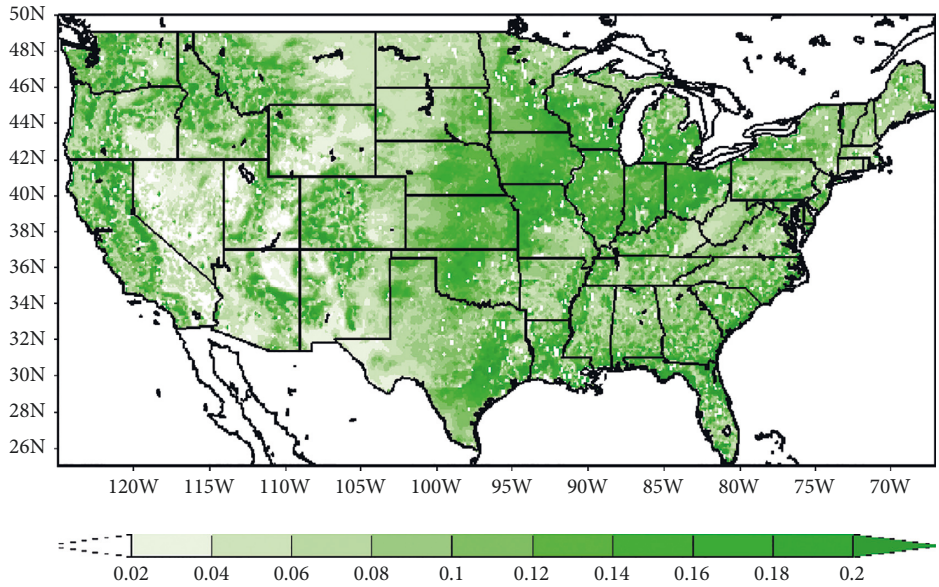

Figure 1: RMSD between climatological and NRT GVF over 2000–2012 period.

land surface globally [24, 25]. The GVF data set covers the study period from 2000 to 2015.

3.2. North American Soil Moisture Database (NASMD). The NASMD, developed and constructed at the Department of Geography's Climate Science Lab at Texas A&M University, provides a harmonized and quality-controlled SM data set for the entire continent of North America from a variety of networks, such as ARM Southern Great Plains, CRN, OK Mesonet, and SNOTEL [26]. More details of NASMD can be found at http://www.soilmoisture.tamu.edu/. This study examined root-mean-square error (RMSE) and time-series correlation of SM values between Noah estimates and in situ observations. The sample size of valid in situ observations affects the significance levels of RMSE and correlation of validation results. Therefore, certain NASMD sites are eliminated if the number of its valid observations is less than 40% of the total sample size of the whole evaluation period. There are eventually 593 NASMD sites in total involved in the validation process in this study.

3.3. Ground Weather Observational Data for WRF Forecast Validation. The ground weather observations including near surface variables and precipitations are assembled to quantify the performance of NUWRF runs with the two different sets of GVF inputs. Specifically, the Global Upper Air and Surface Weather Observations from the National Center for Environmental Prediction (NCEP) are collected for the evaluation of near surface temperature and humidity forecasts. These observations are composed of a global set of surface and upper air reports operationally processed by the NCEP, including pressure, geopotential height, temperature, dew point temperature, and wind direction and speed with the time intervals ranging from hourly to 12 hourly. The data were obtained from the National Center for Atmospheric Research, Computational and Information Systems Laboratory: http://www.rda.ucar.edu/data sets/ds337.0. Additionally, NCEP National Stage IV Precipitation Analysis [27, 28] is used to evaluate precipitation forecasts from each of the WRF runs. Stage IV is a mosaic of regional multisensor analysis product produced by NWS River Forecast Centers. The real-time, 4 km, hourly/6-hourly Stage IV product is collected from the National Center for Atmospheric Research, and further details of the product can be found at http://www.emc.ncep.noaa.gov/mmb/ylin/pcpanl/.

4. Results

4.1. Difference between Climatological and NRT GVF Data Sets. Spatial distribution of root-mean-square difference (RMSD) between climatological and NRT GVF data sets over the CONUS domain averaged for a 13-year period from 2000 to 2012 is shown in Figure 1. In general, these two data sets agree with each other with the mean absolute difference of 0.126 for all land pixels. However, large differences can be observed in the central and eastern agricultural regions, where GVF may change dramatically, especially over the growing season (April to October). The RMSD can be as large as 0.2 in Midwest area, and the long-term variation over western coast area is also significant with RMSD on the order of 0.1 to 0.2. Notably, NRT GVF disagrees to climatology greatly with RMSD more than 0.2 in eastern Texas. RMSD statistics over nearly 600 ground sites from NASMD network show that about 35 percent of sites have seen >20% difference. Among the total of 593 sites, the difference can reach as high as 70% over 14 sites.

4.2. Evaluation of the Noah Off-Line SM Simulations. The significant differences between the climatological and NRT GVF data sets presented in Figure 1 would inevitably impact on SM estimates from Noah LSM. To assess the impact of NRT

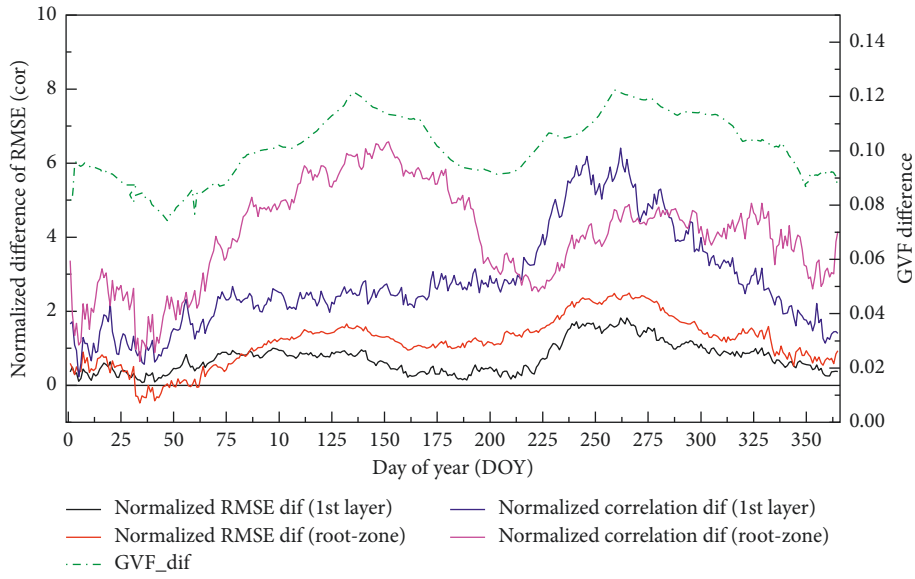

Figure 2: Normalized differences in RMSE and correlations between Noah estimates and in situ observations. Normalized RMSE difference = (RMSE (Noah-clim)−RMSE (Noah-NRT))/RMSE (Noah-clim); normalized correlation difference = (correlation (Noah-NRT)−correlation (Noah-clim))/correlation (Noah-clim); surface and root zone SM are analyzed separately.

satellite-based observations on Noah SM estimates, Noah LSM SM simulations using either the climatological or NRT GVF are compared against in situ SM measurements from a total of 593 NASMD sites over the period of 2000 to 2012.

SM RMSEs of the Noah off-line simulations with climatology and the one with NRT GVF are calculated separately for each day of year, by comparing with in situ SM observations across CONUS domain. To better address the relative impact, the normalized RMSE difference, $(RMSE_{clim}-RMSE_{NRT})/RMSE_{clim}$, is calculated to verify the performance of off-line Noah LSM before and after the utilization of NRT GVF data set. The positive value represents SM estimates when insertion of NRT GVF has less error compared to in situ observations, which represents improvements, and vice versa. Similarly, the normalized difference in time-series correlations, $(COR_{NRT}-COR_{clim})/COR_{clim}$, is examined, with positive (negative) value representing added (degraded) skill with the use of NRT GVF. The normalized difference in RMSEs and correlations is computed for surface and root zone SM estimates separately. The results are shown in Figure 2, along with mean GVF difference at corresponding day of the year, used as a reference.

The differences in RMSEs/correlations illustrate that the insertion of NRT GVF presents overall positive impact on Noah SM estimates for both surface and root zone, except for slight degraded RMSE in root zone SM for a very short period in February (DOY 32 to DOY 63). The Noah model performs better using NRT GVF as inputs, lowering RMSE by around 1.0% (1.18%) and strengthening correlation by 2.80% (4.05%) for surface (root zone) SM estimates on average. According to the curve of GVF differences in Figure 2, climatology and NRT data sets depict large disagreement over two transition stages: (1) green-up phase (DOY 100 to DOY 150) when surface vegetation turns green and (2) senescence phase (DOY 240 to DOY 290) when vegetation coverage decreases sharply. Correspondingly, these are the two periods when NRT GVF insertion impacts the Noah performance most. The RMSE is reduced by about 1.0% (1.41%) during the green-up phase and by 1.48% (2.24%) over the senescence phase for the surface (root zone) SM simulations, and the correlation is enhanced by as much as 5.77% for root zone SM over the green-up period. The result further suggests that larger improvements are gained in root zone SM estimates with additional 0.71% reduction in RMSE and 1.24% enhancement in correlation, compared to those of surface soil moisture.

Worth noting in the pattern of stations showing improvement/degradation is that it matches well with the map of RMSD between climatological and NRT GVF. Taking a closer look at the spatial distribution of normalized RMSE differences in the NRT GVF case in Oklahoma (Figure 3), stations in northwestern Oklahoma where the RMSD is as high as 18% present overall improvement by 2–4% for surface SM estimates and 4–6% for the root zone. On the other hand, stations over southeastern Oklahoma showing less improvement or slight degradation are the ones where small RMSD exists between climatological and NRT GVF. The similar pattern can be found in Nebraska (southern versus upper regions). On top of showing overall improvements over the whole study domain (CONUS), it is promising and even more valuable to see the improvement in LSM SM estimates where the NRT GVF carries more accurate information on the land surface conditions than the static GVF climatology.

4.3. Differences of WRF Forecasts Using Climatological and NRT GVF. Weather forecasts from the WRF model runs using either NRT GVF or GVF climatology are compared with each other to demonstrate the impact of NRT GVF data set. The average GVF difference between NRT GVF and

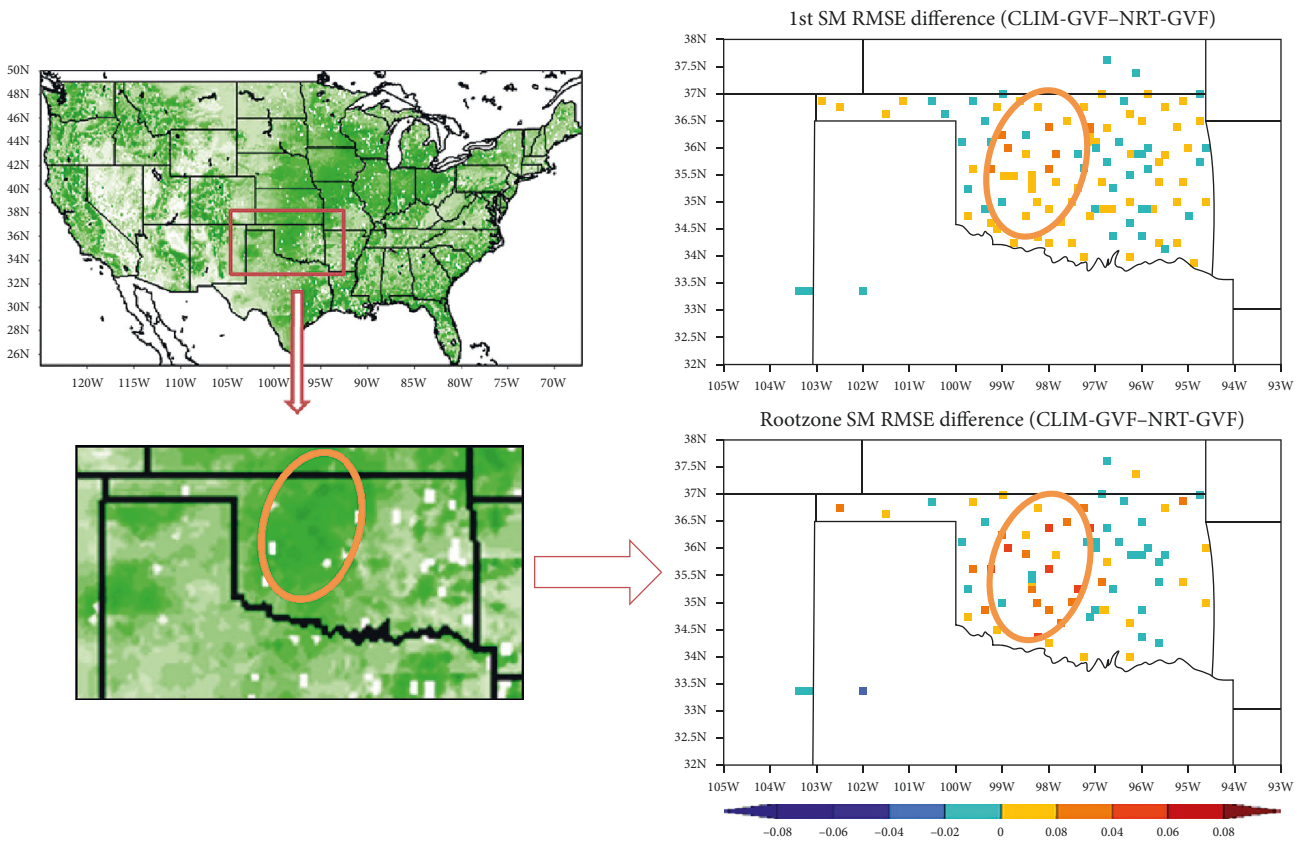

Figure 3: NRT GVF impact to Noah surface and root zone simulations over Oklahoma.

climatology over the period of 3 October–9 October 2015 is shown in Figure 4(a). The NRT data set depicts relatively lower GVF over the most parts of CONUS and substantially higher values over the Northern West Coast and the Gulf of Mexico coastal regions. Largest differences occurred over northern Midwest where NRT GVF was about 20% lower than the GVF climatology. The GVF differences brought substantially changes in WRF model forecasts. The corresponding variations introduced by the change in GVF inputs in top layer soil moisture, surface skin temperature, and 2 m air temperatures at 1900 UTC averaged from 3 October to 9 October 2015 are presented in Figures 4(b)–4(d), respectively. Evidently, the forecasts of skin temperature and 2 m air temperature increased over most of regions from WRF-NRT run, responding to the negative anomaly compared to GVF climatology. The relatively lower NRT GVF in majority of central CONUS resulted in portioning more of net radiation into sensible heat flux, which in turn heated up both skin temperature and 2 m temperature. The results are physically sound as 2 m surface temperature forecast using NRT GVF increased in response to the negative anomaly compared to GVF climatology, and vice versa, in other areas where NRT GVF showed positive anomaly.

4.4. Detailed Evaluation of the WRF Forecasts Using the Different GVF Inputs. To assess the performance of WRF runs with climatology and NRT GVF inputs, WRF model forecasts were further evaluated against ground weather observations from over a thousand ground sites. Specifically, forecasts of 2 m air temperature, 2 m relative humidity, and 24-hour precipitation from WRF-clim and WRF-NRT runs are validated as shown in the following subsections.

4.4.1. T2m: 2-Meter Air Temperature. Figure 5 shows the time-series comparison of 2 m air temperature forecasts from WRF runs with climatology (WRF-clim) and NRT GVF (WRF-NRT) inputs along with the in situ observations averaged over more than thousand ground sites across the CONUS domain from 2 October to 10 October 2015. The validation against the ground observations illustrates that WRF-clim run predicted 2 m temperature forecasts with an overall cold bias during the daytime and warm bias over nighttime throughout the validation period. The bias reaches 2.46 K at daytime and 0.58 K at nighttime averaged from all validation sites over CONUS. Notably, the use of NRT GVF as model input reduced the cold bias by 0.43° on average. However, less impact and even slightly degradation occurred to nighttime forecasts. It is worth mentioning that the improvement of 0.43° at daytime is an average from all validation sites across CONUS (approximately a thousand sites). When breaking down the results into subregions, the magnitude of impact is substantially higher. Forecasts of 2 m surface air temperature from WRF runs compared with in situ observations, averaged from validation sites over the LMV subregion (around 200 sites), are presented in Figure 6. Similar conclusion can be drawn that improvement is

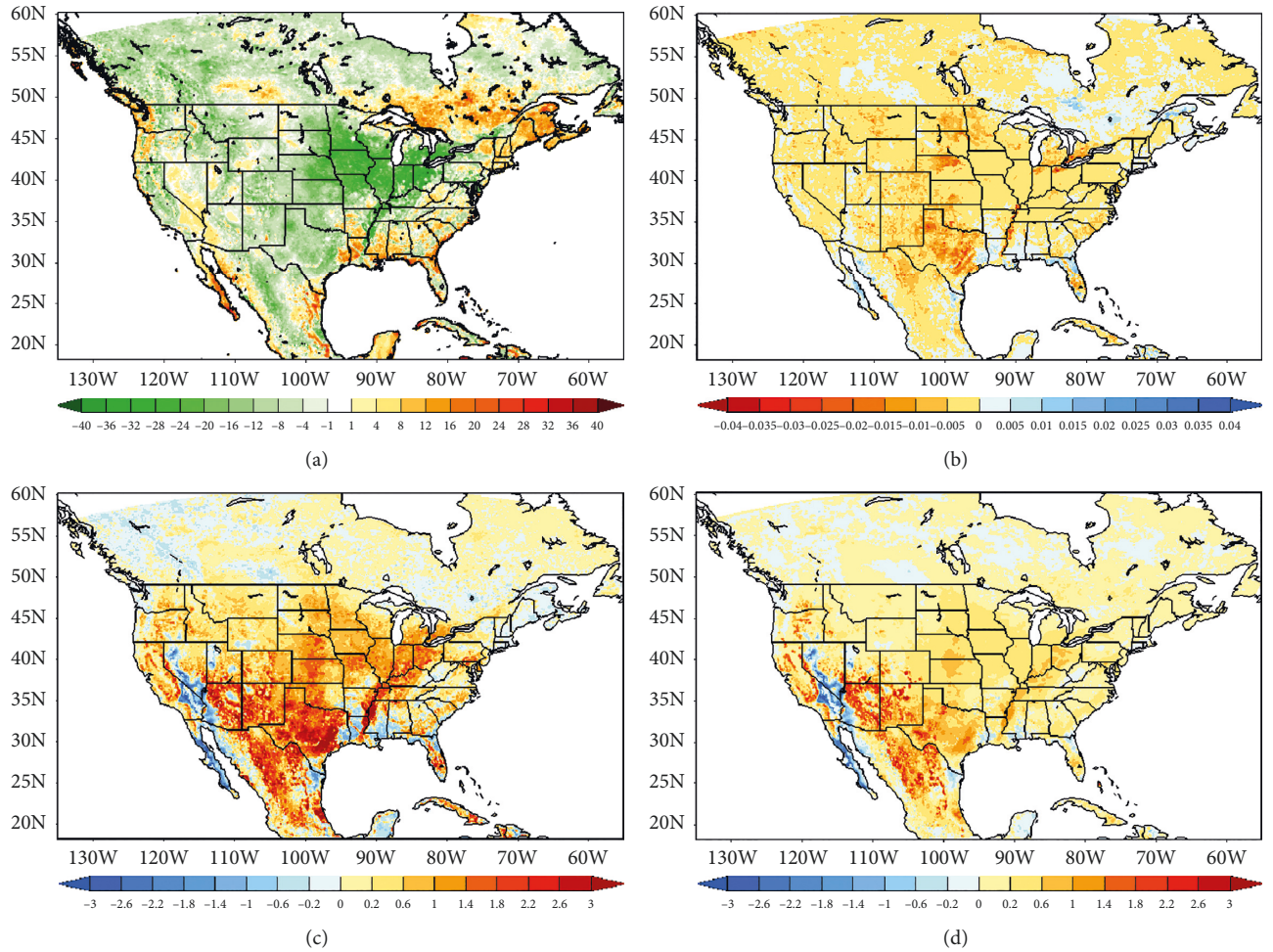

Figure 4: Differences of the WRF-NRT and WRF-Clim runs averaged from 3 October–9 October 2015: (a) GVF input (ΔGVF); (b) top-layer soil moisture output (ΔSM1); (c) skin temperature forecast (ΔTskin); (d) 2 m surface air temperature forecast (ΔT2m).

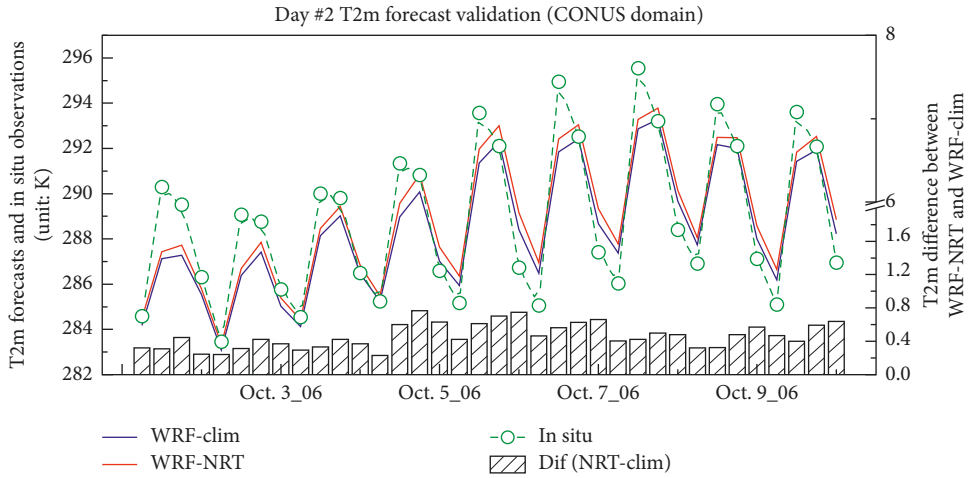

Figure 5: Comparison of 2 m surface air temperature forecasts between WRF runs (with climatology and NRT GVF) and in situ observations; T2m averaged from all validation sites over CONUS.

obtained by the insertion of NRT GVF. The use of NRT GVF as input reduced the daytime cold bias by 0.8 K on average, with very large impact of corrected bias on the order of 1.0 K to 1.7 K from 5 October to 7 October. The validation results are then shown separately for Day 1 (top) and Day 2 (bottom) forecasts in Figure 7. Although the biases shown in

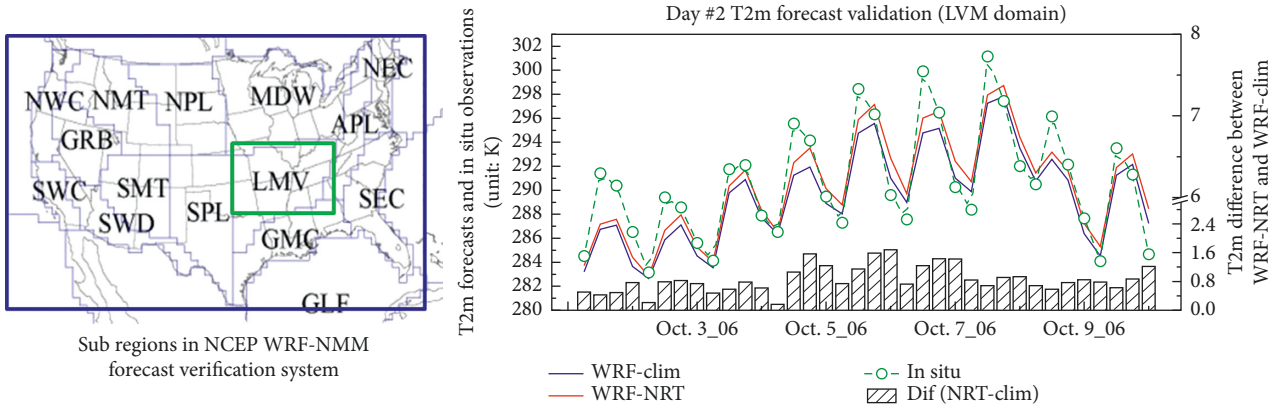

FIGURE 6: Forecasts of 2 m surface air temperature from WRF runs (with climatology and NRT GVF) along with in situ observations, averaged from validation sites over LMV subregion.

both day's forecasts are in similar pattern (cold bias at daytime and warm bias at nighttime), it is worth noting that the bias on Day 2 forecast is generally larger than that on Day 2 by 0.37° on average. It is reasonable and understandable that the errors can be accumulated along the time in the WRF predictions.

Maps of the differences in RMSEs for each of the validation sites are capable of presenting improvement/degradation from a spatial perspective. Spatial distribution of validation results is presented here over a total of 1178 ground sites collected from the Global Upper Air and Surface Weather Observations. The spatial distribution of the differences in RMSE of 2 m temperature forecast between WRF-clim and WRF-NRT runs during the daytime is shown in Figure 8. The RMSE difference is calculated by WRF-clim run minus WRF-NRT runs, with positive (negative) values meaning that forecasts from control run showing larger (smaller) error than that using NRT GVF. The sites with warm (cool) color shown in the map are where the data assimilation presents the added (degraded) value in the 2 m temperature forecasts. Evidently, around 82.3% validation sites (out of 1178 sites) showed positive impact with the insertion of NRT GVF.

4.4.2. RH: 2-Meter Relative Humidity. The impact of NRT GVF on WRF model humidity forecasts is also evaluated using ground observations. Figure 9 exhibits the 2 m relative humidity (RH2m) forecasts between WRF runs (with climatology and NRT GVF) and in situ observations averaged from all validation sites over the CONUS domain for the period from 1 October to 10 October 2015. WRF-clim run presents a consistently positive bias compared to the in situ measurements. The time-series comparison suggests that the insertion of NRT GVF is able to reduce the positive bias by 1.63% on average over the 10-day validation period. Similarly to the analysis in near surface temperature, the spatial distribution of the difference in RMSE of RH2m forecasts is checked for more than 1000 validation sites over the CONUS domain (not shown in the paper). The positive impact with the insertion of NRT GVF is gain over majority of the validation sites, which is consistent with the conclusion from 2 m temperature validation.

4.4.3. P: Daily Precipitation. WRF model precipitation forecasts (with climatology and NRT GVF inputs) were evaluated by comparing them with the National Stage IV Precipitation data set grid by grid. The RMSE and correlation (Figure 10) are calculated for WRF-clim and WRF-NRT runs separately, relative to Stage IV precipitation analysis. The smaller RMSE and higher correlation coefficient averaged over the CONUS domain illustrated marginal improvement in precipitation forecasts from WRF using the NRT GVF. The WRF precipitation forecasts using WRF-NRT aligned more closely with the Stage IV analysis especially on 4, 5, and 6 October 2015, compared to the WRF-clim run.

5. Discussion and Summary

While green vegetation fraction is a critical input parameter to the NOAA NCEP operational Noah land surface model and NWP models and near real-time observations from VIIRS on Suomi NPP and JPSS satellites are or will be stably available, current NCEP Noah LSM and NWP models are still using the multiyear averages of monthly GVF data set from the old NOAA AVHRR observations. The old GVF data set may not be representative to the real-time situation of land surface vegetation cover. This land vegetation cover input directly impacts the energy balance of land surface, and thus, accurate information of the parameter could be critical to the accuracy of model forecasts. This study attempted to improve estimates from off-line models and forecasts from the numerical weather prediction model by using the NRT satellite-based GVF data products. The comprehensive analysis on the impacts of NRT GVF on both off-line LSM and NWP models is carried out.

The magnitude of differences between climatology and NRT GVF was quantitatively evaluated. Statistics indicated that significant variation exists between climatology and NRT GVF with the average difference of 12.6% over the CONUS domain, and large difference on the order of 14% to 20% can be detected in central and eastern regions. The significant differences of the NRT GVF compared to multiyear climatology were expected to affect the forecasts of the Noah land surface model and consequently the NCEP NWP model forecasts as well.

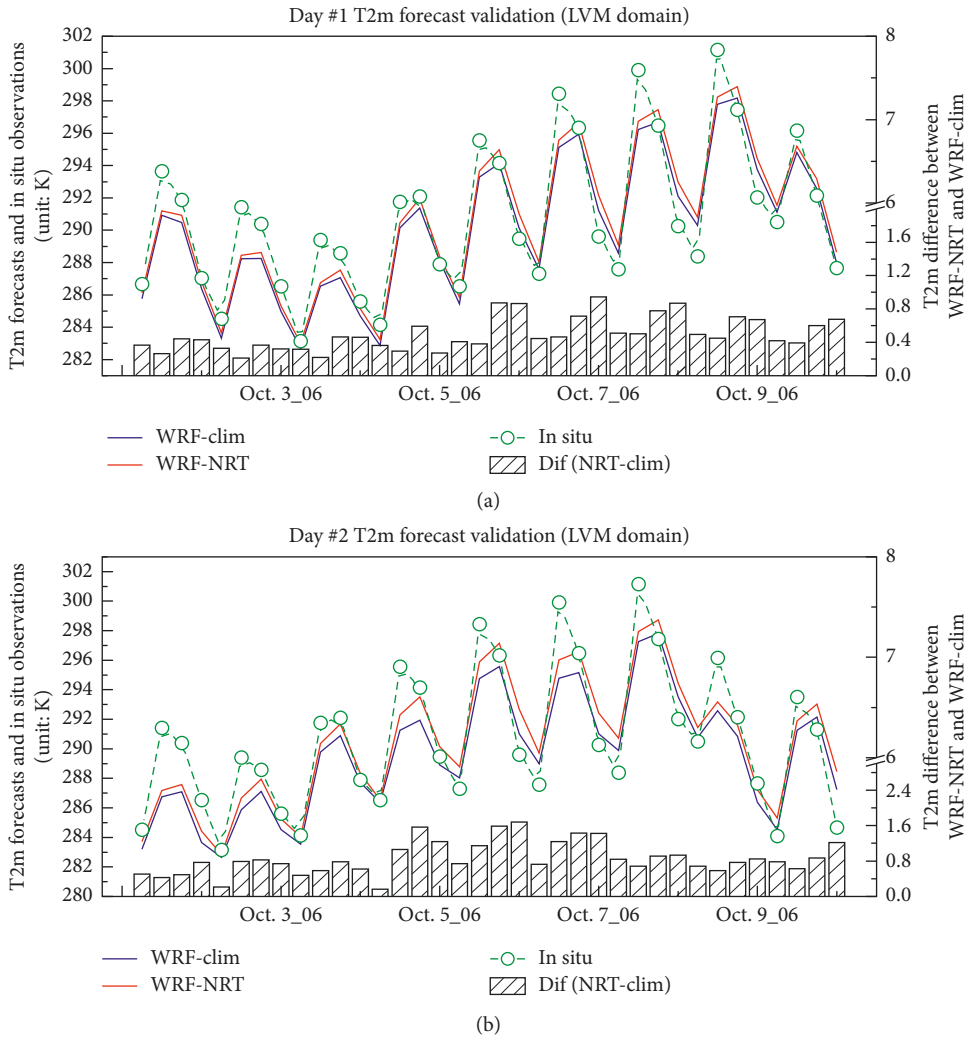

Figure 7: Forecasts of 2 m surface air temperature from WRF runs (with climatology and NRT GVF) along with in situ observations for Day 1 forecasts (a) and Day 2 forecasts (b), averaged from validation sites over LMV subregion.

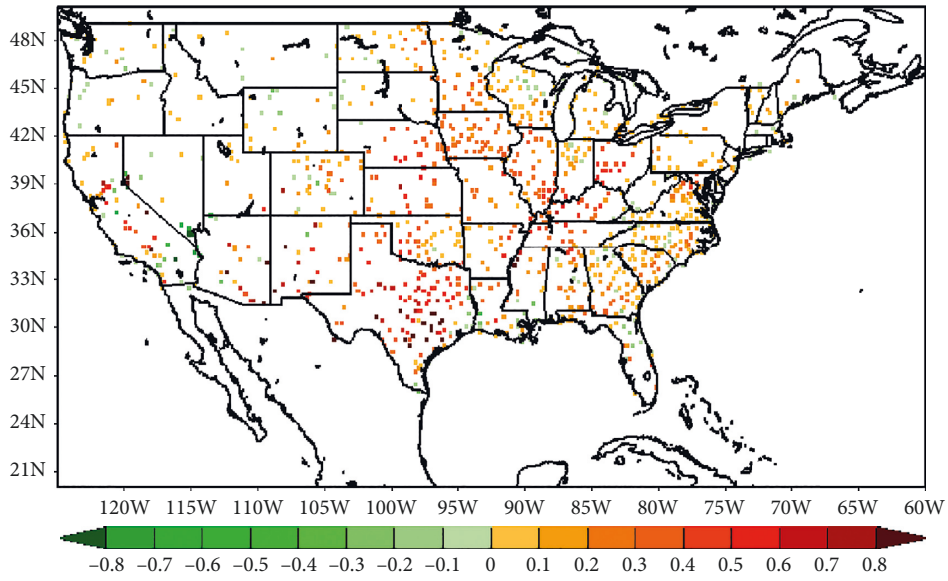

Figure 8: Difference in RMSE of T2m forecasts between WRF run with GVF climatology and one with NRT GVF during the daytime; WRF-clim run minus WRF-NRT run; warm (cool) color means the added (degraded) value.

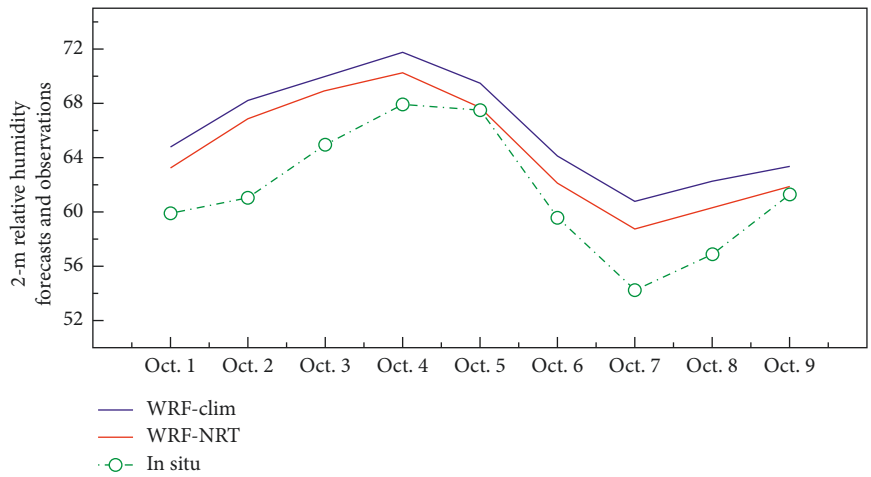

Figure 9: Comparison of 2 m relative humidity (RH2m) forecasts between WRF runs (with climatology and NRT GVF) and in situ observations; RH2m averaged from all validation sites over CONUS.

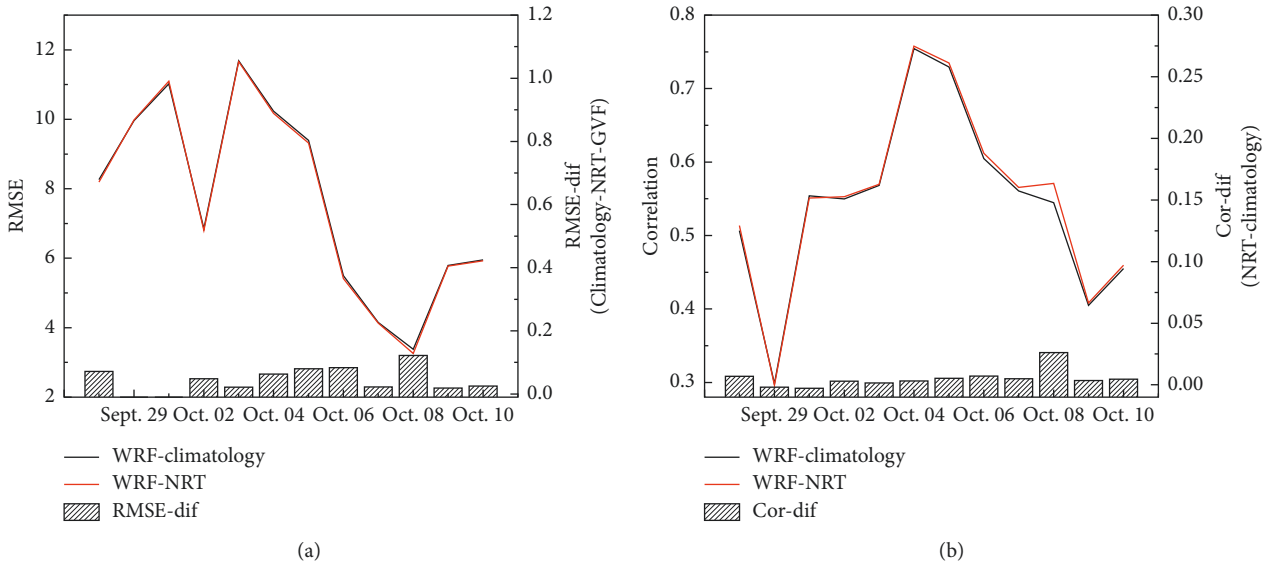

Figure 10: Comparison of RMSE (a) and correlation coefficient (b) of 24 h accumulated precipitation forecasts from WRF runs using climatological and NRT GVF during 3 October–10 October 2015.

Impacts of introducing NRT GVF into off-line Noah LSM were evaluated based on a 13-year period analysis from 2000 to 2012. The RMSE and correlation coefficient between Noah SM estimates and in situ SM observations from 593 NASMD sites were examined from temporal and spatial perspectives. Validation results indicated that (1) SM estimates from the Noah model using NRT GVF were more closely agreed with in situ observations, compared to those using multiyear-averaged GVF. (2) NRT GVF insertion was shown to provide significant improvement on the SM estimates particularly over green-up and senescence phases, with RMSE (correlation) reduced (enhanced) by around 2.24% (5.77%) for root zone simulations on average. These two transition stages are periods when NRT GVF differs from climatology product most (Figure 1) and impacts of NRT GVF are all positive in terms of bias, RMSE, and correlation. (3) The spatial pattern of validation stations with improvement matches well with that of GVF RMSD, where higher RMSD in GVF leads to bigger improvement (examples in Oklahoma; Figure 3). Therefore, on top of showing overall improvements over the whole study domain (CONUS), it is promising and even more valuable to see the improvement in LSM SM estimates where the NRT GVF captures more accurate surface vegetation signals than the static GVF climatology. (4) With the replacement of NRT GVF, improvements were gained for both top layer and root zone SM estimates, while larger improvements were found in root zone SM estimates with additional ~1% reduction in RMSE and 1.24% enhancement in correlation. The impact on root zone SM is of a great value because it may provide broader benefits to data users and applications like drought monitoring.

The value of NRT GVF in forecasts of the WRF model was examined by comparing WRF air temperature, relative

humidity, and precipitation forecasts (with climatology and NRT GVF) with in situ observations over nearly thousand ground sites. WRF model forecasts of 2 m air temperature and relative humidity using NRT GVF showed a better agreement with the ground weather observations in general with smaller RMSEs and higher correlation coefficients. Verification results show the use of NRT GVF as input reduced the daytime cold bias of T2m by 0.8 K on average, with very large impact of corrected bias on the order of 1.0 K to 1.7 K. Additionally, the time-series comparison of RH2m suggests that the insertion of NRT GVF is able to reduce the bias by 1.63% on average. Using the NRT GVF in Noah LSM is helpful to reduce WRF model forecast bias significantly.

Marginal improvement in WRF model precipitation forecasts was found using the NRT GVF. It is more challenging to demonstrate significant impact on precipitation forecasts by assimilating land surface variables, compared to the near surface forecasts, for example, T2m and RH2m, especially over the short time period. Future research may involve a fully coupled land data assimilation utility with the WRF model, which would better response to the land and atmospheric interaction.

In conclusion, using near real-time GVF in Noah land surface model showed significant impact on predictions of both off-line Noah LSM and WRF models. With the high quality and easily accessible satellite-based near real-time GVF observations, the NCEP Noah land surface model soil moisture estimates and WRF model forecasts are expected to be improved. Switching the old GVF data set to the near real-time satellite observations could benefit the NCEP weather forecast operations.

Data Availability

The data used to support the findings of this study are available from the corresponding author upon request.

Conflicts of Interest

The authors declare that there are no conflicts of interest regarding the publication of this paper.

Acknowledgments

The authors would like to thank the following three programs for their partial supports to this study: NOAA NESDIS GOES-R Risk Reduction Program (GOES-R3), NOAA NESDIS JPSS Proving Ground and Risk Reduction Program (JPSS PGRR), and NOAA Climate Program Office Modeling, Analysis, Prediction, and Projections (MAPP) program. They would also like to thank Dr. Gao Feng of USDA for providing smoothed and gap-filled MODIS LAI software package.

References

[1] R. D. Koster, "The components of a "SVAT" scheme and their effects on a GCM's hydrological cycle," *Advances in Water Resources*, vol. 17, no. 1-2, pp. 61–78, 1994.

[2] F. Chen, K. Mitchell, J. Schaake et al., "Modeling of land surface evaporation by four schemes and comparison with FIFE observations," *Journal of Geophysical Research*, vol. 101, no. 3, pp. 7251–7268, 1996.

[3] E. F. Wood, D. Lettenmaier, X. Liang, B. Nijssen, and S. W. Wetzel, "Hydrological modeling of continental-scale basins," *Annual Review of Earth and Planetary Sciences*, vol. 25, pp. 279–300, 1997.

[4] K. Mitchell, D. Lohmann, P. R. Houser et al., "The multi-institution North American Land Data Assimilation System (NLDAS): utilizing multiple GCIP products and partners in a continental distributed hydrological modeling system," *Journal of Geophysical Research*, vol. 109, no. 7, 2004.

[5] V. I. Koren, M. Smith, D. Wang, and Z. Zhang, "Use of soil property data in the derivation of conceptual rainfall-runoff model parameters," in *Proceedings of the 15th Conference on Hydrology*, pp. 103–106, Long Beach, CA, USA, January 2000.

[6] F. N. Kogan, "Global drought watch from space," *Bulletin of the American Meteorological Society*, vol. 78, no. 4, pp. 621–636, 1997.

[7] F. Abramopoulos, "Generalized energy and potential enstrophy conserving finite-difference schemes for the shallow-water equations," *Monthly Weather Review*, vol. 116, no. 3, pp. 650–662, 1988.

[8] G. Gutman and A. Ignatov, "The derivation of the green vegetation fraction from NOAA/AVHRR data for use in numerical weather prediction models," *International Journal of Remote Sensing*, vol. 19, no. 8, pp. 1533–1543, 1998.

[9] I. Csiszar and G. Gutman, "Mapping global land surface albedo from NOAA AVHRR," *Journal of Geophysical Research: Atmospheres*, vol. 104, no. 6, pp. 6215–6228, 1999.

[10] J. Yin, X. Zhan, Y. Zheng et al., "Improving Noah land surface model performance using near real time surface albedo and green vegetation fraction," *Agricultural and Forest Meteorology*, vol. 218, pp. 171–183, 2016.

[11] R. L. Ruhge and M. Barlage, "Integrating a real-time Green Vegetation Fraction (GVF) Product into the Land Information System (LIS)," in *Proceedings of the 15th Symposium on Integrated Observing and Assimilation Systems for Atmosphere, Oceans, and Land Surface*, Seattle, WA, USA, pp. 1–12, 2011.

[12] L. Jiang, F. N. Kogan, W. Guo et al., "Real-time weekly global green vegetation fraction derived from advanced very high resolution radiometer-based NOAA operational global vegetation index (GVI) system," *Journal of Geophysical Research*, vol. 115, no. 11, 2010.

[13] K. A. James, D. J. Stensrud, and N. Yussouf, "Value of real-time vegetation fraction to forecasts of severe convection in high-resolution models," *Weather and Forecasting*, vol. 24, no. 1, pp. 187–210, 2009.

[14] J. Miller, M. Barlage, X. Zeng, H. Wei, K. Mitchell, and D. Tarpley, "Sensitivity of the NCEP/Noah land surface model to the MODIS green vegetation fraction data set," *Geophysical Research Letters*, vol. 33, no. 13, 2006.

[15] F. Chen and J. Dudhia, "Coupling an advanced land surface-hydrology model with the Penn State-NCAR MM5 Modeling system. part I: model implementation and sensitivity," *Monthly Weather Review*, vol. 129, no. 4, pp. 569–585, 2001.

[16] S. V. Kumar, C. D. Peters-Lidard, Y. Tian et al., "Land information system: an interoperable framework for high resolution land surface modeling," *Environmental Modelling and Software*, vol. 21, no. 10, pp. 1402–1415, 2006.

[17] S. V. Kumar, R. H. Reichle, C. D. Peters-Lidard et al., "A land surface data assimilation framework using the land

information system: description and applications," *Advances in Water Resources*, vol. 31, no. 11, pp. 1419–1432, 2008.

[18] M. B. Ek, K. E. Mitchell, Y. Lin et al., "Implementation of Noah land surface model advances in the National Centers for Environmental Prediction operational mesoscale Eta model," *Journal of Geophysical Research: Atmospheres*, vol. 108, no. 22, p. 8851, 2003.

[19] K. Mitchell, "The community Noah land-surface model: user guide public release on the climate forecast system reanalysis and ensemble NLDAS," *Journal of Hydrometeorology*, vol. 12, no. 2, pp. 185–210, 2005.

[20] C. D. Peters-Lidard, E. M. Kemp, T. Matsui et al., "Integrated modeling of aerosol, cloud, precipitation and land processes at satellite-resolved scales," *Environmental Modelling and Software*, vol. 67, pp. 149–159, 2015.

[21] Y. Xia, "Continental-scale water and energy flux analysis and validation for the North American Land Data Assimilation System project phase 2 (NLDAS-2): 1. Intercomparison and application of model products," *Journal of Geophysical Research*, vol. 117, no. 3, 2012.

[22] Y. Xia, "Continental-scale water and energy flux analysis and validation for North American Land Data Assimilation System project phase 2 (NLDAS-2): 2. Validation of model-simulated streamflow," *Journal of Geophysical Research*, vol. 117, no. 3, 2012.

[23] J. M. Norman, W. P. Kustas, and K. S. Humes, "A two-source approach for estimating soil and vegetation energy fluxes from observations of directional radiometric surface temperatures," *Agricultural and Forest Meteorology*, vol. 77, no. 3-4, pp. 263–293, 1995.

[24] Y. Knyazikhin, J. V. Martonchik, R. B. Myeni, D. J. Diner, and S. W. Running, "Synergistic algorithm for estimating vegetation canopy leaf area index and fraction of absorbed photosynthetically active radiation from MODIS and MISR data," *Journal of Geophysical Research*, vol. 103, no. 24, pp. 32257–32274, 1998.

[25] Y. Knyazikhin, J. Glassy, J. L. Privette et al., *MODIS Leaf Area Index (LAI) and Fraction of Photosynthetically Active Radiation Absorbed by Vegetation (FPAR) Product (MOD15)*, Algorithm Theoretical Basis Document, NASA Goddard Space Flight Center, Greenbelt, MD, USA, 1999.

[26] S. M. Quiring, "Building the North American Soil Moisture (NASM) database," in *Proceedings of the Fall Meeting of the American Geophysical Union*, San Francisco, CA, USA, December 2011.

[27] Y. Lin and K. E. Mitchell, "The NCEP Stage II/IV hourly precipitation analyses: development and applications," in *Proceedings of the 19th Conference on Hydrology, American Meteorological Society*, San Diego, CA, USA, January 2005.

[28] M. E. Baldwin and K. E. Mitchell, "Progress on the NCEP hourly multi-sensor U.S. precipitation analysis for operations and GCIP research," in *Proceedings of the 2nd Symposium on Integrated Observing Systems, 78th AMS Annual Meeting*, Boston, MA, USA, 1998.